

Study of the data taking strategy for a high precision τ mass measurement^{*}

WANG You-Kai(王由凯)^{1,2} ZHANG Jian-Yong(张建勇)^{1:1)}

MO Xiao-Hu(莫晓虎)^{1:2)} YUAN Chang-Zheng(苑长征)¹

1 (Institute of High Energy Physics, CAS, Beijing 100049, China)

2 (School of Physics, Peking University, Beijing 100871, China)

Abstract To achieve a high precision τ mass measurement at the high luminosity experiment BESIII, Monte Carlo simulation and sampling technique are utilized to simulate various data taking cases for single and multi-parameter fits by virtue of which the optimal scheme is determined. The optimized proportion of luminosity distributed at selected points and the relation between precision and luminosity are obtained. In addition, the optimization of the fit scheme is confirmed by scrutinizing a variety of fit possibilities.

Key words τ mass, statistical optimization, luminosity and accuracy

PACS 14.60.Fg

1 Introduction

Because of its relatively large mass and comparatively simple decay mechanism, the τ lepton offers many interesting possibilities for testing and improving the Standard Model (SM). However, as a fundamental parameter in SM, the accuracy of τ mass (m_τ) which is at the level of 10^{-4} for the time being, is around four orders of magnitude lower than that of the other two leptons, electron and muon. Therefore, the accurate measurement of m_τ is still of great importance for τ physics. Usually, the pseudomass technique^[1, 2] and the threshold scan method are employed to measure the m_τ . The former relies on the reconstruction of the invariant mass and energy of the hadronic system in hadronic τ decays while the latter needs a good understanding of the production cross section near threshold.

More than fifteen years ago, the most accurate measurement of m_τ was obtained by BES collaboration^[3–5] using the threshold scan method. Recently, the developments of experimental

techniques^[6] and theoretical calculations^[7–10] have provided the possibility of measuring m_τ with unprecedented accuracy. Moreover, large τ data are expected from the upgraded detector BESIII^[11], therefore, it is of great interest to know what accuracy of m_τ we can expect in the near future.

We devote this paper to the statistical aspect of m_τ measurement. Monte Carlo simulation and sampling technique are employed to simulate various data taking cases for one-, two-, and three-parameter fit schemes. The optimal scheme is determined from the comparison of different kinds of results and the validity of optimization is confirmed by scrutinizing a variety of possibilities. The optimized proportion of luminosity distributed at selected points and the dependence of precision on luminosity are obtained to provide numerical information for actual data taking.

2 Methodology

For the experiment using the scan method, several points, say totally N_{pt} points, need to be taken

Received 6 November 2008, Revised 23 December 2008

^{*} Supported by National Natural Science Foundation of China (10491303, 10775142, 10825524), Instrument Developing Project of Chinese Academy of Sciences (YZ200713), Major State Basic Research Development Program (2009CB825206) and Knowledge Innovation Project of Chinese Academy of Sciences (KJCX2-YW-N29)

1) E-mail: jy Zhang@mail.ihep.ac.cn

2) E-mail: moxh@mail.ihep.ac.cn

©2009 Chinese Physical Society and the Institute of High Energy Physics of the Chinese Academy of Sciences and the Institute of Modern Physics of the Chinese Academy of Sciences and IOP Publishing Ltd

in the vicinity of m_τ threshold. By virtue of the analyzed data, the following likelihood function is constructed^[3–5]:

$$LF = \prod_i^{N_{\text{pt}}} \frac{\mu_i^{N_i} e^{-\mu_i}}{N_i!}, \quad (1)$$

where N_i is the number of observed $\tau^+\tau^-$ events obtained by $e\mu$ -tagged final state¹⁾ at the i -th scan point. Here N_i is assumed obeying Poisson distribution, whose expectation μ_i is given by

$$\mu_i(m_\tau) = [\epsilon \cdot B_{e\mu} \cdot \sigma_{\text{obs}}(m_\tau, E_{\text{cm}}^i) + \sigma_{\text{BG}}] \cdot \mathcal{L}_i. \quad (2)$$

In Eq. (2), \mathcal{L}_i is the integrated luminosity at the point i ; ϵ is the overall efficiency of $e\mu$ final state for identifying $\tau^+\tau^-$ events, which includes trigger efficiency and event reconstruction and selection efficiency; $B_{e\mu}$ is the combined branching ratio for decays $\tau^+ \rightarrow e^+\nu_e\bar{\nu}_\tau$ and $\tau^- \rightarrow \mu^-\bar{\nu}_\mu\nu_\tau$, or the corresponding charge conjugate mode; σ_{obs} (with m_τ as one of parameters), which can be calculated by the improved Voloshin's formulas^[7], is the observed cross section measured at the point i with energy E_{cm}^i ; and σ_{BG} is the total cross section of background channels after $\tau^+\tau^-$ selection. If m_τ is set as a free parameter, the maximization of LF in Eq. (1) yields the best estimation for m_τ .

As a statistical study, the aim is to discover the scheme which can provide the highest precision on m_τ for a specified period of data taking time or equivalently for a given integrated luminosity. To this end, the sampling technique is utilized to simulate various data taking schemes and/or possibilities among which the optimal one is chosen. For a special scheme, N_i is sampled according to Poisson distribution and μ_i is calculated firstly by Eq. (2), where the following values are taken: $m_\tau = 1776.99$ MeV, $B = 0.06194$ ^[12], $\epsilon = 14.2\%$, and $\sigma_{\text{BG}} = 0.024$ pb^[4]. As to E_{cm}^i and \mathcal{L}_i , they vary with distinctive simulated schemes. As a special strategy²⁾, the energy interval to be studied is divided evenly:

$$E_i = E_0 + (i-1) \times \delta E, \quad (i = 1, 2, \dots, N_{\text{pt}}) \quad (3)$$

where the initial point $E_0 = 3.50$ GeV, the final point $E_f = 3.595$ GeV, and the fixed step $\delta E = (E_f - E_0)/N_{\text{pt}}$ with N_{pt} being the number of energy points. For a given integrated luminosity (\mathcal{L}_{tot}) it is also apportioned averagely at each point, that is $\mathcal{L}_i = \mathcal{L}_{\text{tot}}/N_{\text{pt}}$.

In actual fit, besides m_τ , the other parameters can also be set free and determined from maximization of

LF in Eq. (1). In the following study, one parameter m_τ is set free firstly, then two parameters m_τ and ϵ ; at last, three parameters m_τ , ϵ , and σ_{BG} . For three-parameter fit, the low bound of $\sigma_{\text{BG}} \geq 0$ is added from the physics point of view. In each fit, the fixed parameters take the values used in the simulation.

For each special scheme (that is for each N_{pt}), in order to reduce the statistical fluctuation, sampling is repeated many times ($N_{\text{samp}}=200$ in this paper), the average value and corresponding variance of the fit out variables are worked out as follows^[13]:

$$\bar{X}^i = \frac{1}{N_{\text{samp}}} \sum_{j=1}^{N_{\text{samp}}} X_j^i, \quad (4)$$

$$S_X^2(X^i) = \frac{1}{N_{\text{samp}} - 1} \sum_{j=1}^{N_{\text{samp}}} (X_j^i - \bar{X}^i)^2. \quad (5)$$

where X denotes the free fitting parameter which can be m_τ , ϵ , and/or σ_{BG} . Here it should be noted that i indicates a certain scheme, whose value can be 1 while j indicates the sampling times which equals 200 in the following study. Without special declaration, the meaning of the average defined by Eqs. (4) and (5) will be kept in the following study. The general flow chart of sampling and fitting research is presented in Fig. 1.

In the process of statistical research, we want to figure out the following issues:

- 1) Number of points to be taken;
- 2) Optimal position of the selected points;
- 3) Dependence of the required precision on the needed luminosity.

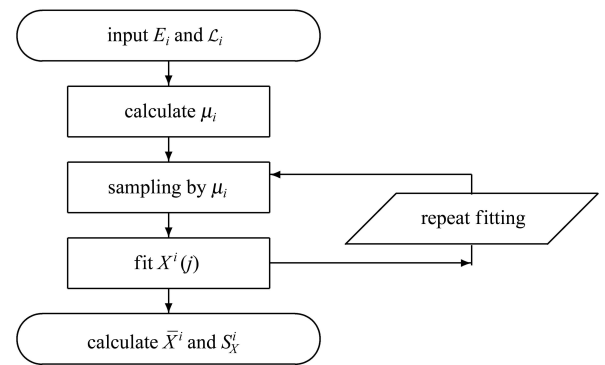


Fig. 1. The flow chart of sampling simulation, where i ($i = 1, 2, \dots, N_{\text{pt}}$) indicates certain scheme and j ($j = 1, 2, \dots, N_{\text{samp}}$) sampling times.

1) For brevity, the $e\mu$ channel means $\tau^+ \rightarrow e^+\nu_e\bar{\nu}_\tau$, $\tau^- \rightarrow \mu^-\bar{\nu}_\mu\nu_\tau$, and/or its charged conjugate mode $\tau^- \rightarrow e^-\bar{\nu}_e\nu_\tau$, $\tau^+ \rightarrow \mu^+\nu_\mu\bar{\nu}_\tau$.

2) In fact, there may be many strategies to design various data taking schemes. Moreover, the number of data taken points depends on the distribution of points, and vice versa. Anyway, in the following study, it is found that one parameter can usually be determined by one point. Therefore, it is enough to merely adopt one kind of strategies for data taking design.

3 Optimization

3.1 Conclusion of the one-parameter fit

The one-parameter fit has been studied meticulously in Ref. [14] and merely recapitulated here are the conclusions. When m_τ is the only fit parameter, the research reveals that

1. The optimal position for data taking is located at the region near the $\tau^+\tau^-$ production threshold with large derivative of the $e^+e^- \rightarrow \tau^+\tau^-$ cross section to energy;

2. One point is enough to achieve small error within the optimal region;

3. The empirical formula of the relation between fit uncertainty S_{m_τ} and luminosity \mathcal{L} can be fitted based on the data provided in Ref. [14] as follows

$$S_{m_\tau}[\text{keV}/c^2] = \frac{708.05}{\mathcal{L}^{0.504}[\text{pb}^{-1}]}, \quad (6)$$

which indicates that 49 pb^{-1} is sufficient for a statistical precision better than $0.1 \text{ MeV}/c^2$.

The conclusions listed here are easy to understand. First, since there is only one free parameter (m_τ) needed to be fit in the $\tau^+\tau^-$ production cross section, one measurement will fix the shape of the curve. Second, the fitted parameter will be sensitive to the variation of curve. Mathematically, the variation of curve can be described by its derivative. So the sensitive point for m_τ will be in the region with large derivative.

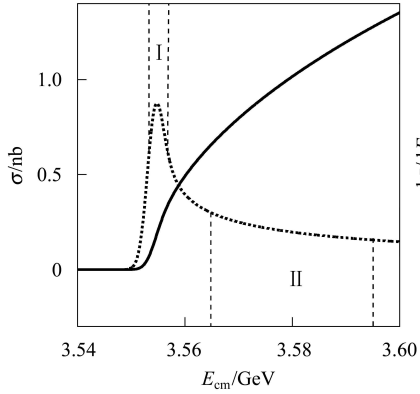


Fig. 2. Two subregions, denoted by I and II, with different derivative features where the solid line denotes the observed cross section and the dashed line the corresponding derivative value with a scale factor of 10^{-2} .

More remarks are in order here. In Ref. [14] (as shown in Fig. 2), two regions are selected: the region I ($E_{\text{cm}} \subset (3.553, 3.558) \text{ GeV}$) is selected where the derivative falls to 75% of its maximum while the region II ($E_{\text{cm}} \subset (3.565, 3.595)^{1)} \text{ GeV}$) is selected where the variation of derivative is comparatively smoother than that in region I. In region I, the variation of derivative against the energy is fairly prominent which indicates that such a region will be sensitive to the horizontal change (that is the change of energy scale). Therefore, region I is optimal for m_τ which is determined by both the shape of the cross section curve and the energy scale. Comparatively, the variation of derivation in region II is smooth, so it is insensitive to the horizontal change but can be sensitive to the vertical change. That is to say, it could be expected that region II will be optimal for efficiency which determines the overall normalization of the curve. This guess will be proved by our following study relevant to the two-parameter fit.

3.2 Two-parameter fit

In the light of the results of the one-parameter fit, the first point is fixed at τ threshold ($E_1 = 3.55379 \text{ GeV}$) to determine the parameter m_τ . As to the new adding fit parameter ϵ , half of the luminosity 100 pb^{-1} is divided evenly into N_{pt} points ($N_{\text{pt}} = 1, 2, \dots, 20$) within the energy region suggested in one-parameter fit ($E_{\text{cm}} \subset (3.565, 3.595) \text{ GeV}$). To determine optimal N_{pt} , m_τ is fixed and the only parameter ϵ is fit. The results are shown in Fig. 3(a) by virtue of which we note two points: first, the absolute value of S_ϵ is much larger than that of $\Delta\epsilon$, so from the point view of accuracy, the former is much more crucial than the latter. Therefore, S_ϵ is adopted to access the fit quality of parameter ϵ . Second, it is obvious that one point (denoted as the second point, E_2 , hereafter) is enough to afford the smallest fit uncertainty for ϵ .

Then with the increasing energy position, the fit is performed to find optimal position for E_2 . Fig. 3(b) shows the distributions of S_{m_τ} and S_ϵ with the variation of the second point. Also shown are the cross section and its derivative to energy. It is obvious that the S_ϵ decreases with the decreasing of the derivative. Therefore, the optimal position of E_2 can be selected far from the τ threshold at the high energy side, for example $E_2 = 3.595 \text{ GeV}$.

1) In fact, the region II could be selected further away from τ threshold. But as indicated from the following simulation, the uncertainty of τ mass remains almost the same when the upper energy point greater than 3.58 GeV . Therefore the upper-limit of the scan is not crucial for our further study, that is to say, the upper-limit could be selected with large freedom, such as $3.59, 3.595, 3.6, 3.605 \text{ GeV}$, and so on. Anyway, when the energy is greater than 3.65 GeV the effect due to $\psi(2S)$ resonance will exhibit. Therefore, the upper-limit of τ mass scan should be less than 3.65 GeV .

Unlike the one-parameter fit, besides finding the relation between luminosity and precision, it is also necessary to know the luminosity allocation between the first and second points. To this end, for certain total luminosity, say $L_{\text{tot}} = 100 \text{ pb}^{-1}$, the distinctive allocation schemes are checked and the results are displayed in Fig. 3(c). Just as expected, with the increasing of L_1 (decreasing of L_2), S_{m_τ} (S_ϵ) decreases (increases) correspondingly. The abnormal increasing of S_{m_τ} at the extreme region where L_2 is almost zero, can be explained as the correlation effect between S_{m_τ} and S_ϵ . By virtue of the curve from fitting the data in Fig. 3(c), the minimal value of S_{m_τ} can be figured out as 0.75, or equivalently $L_1 : L_2 = 3 : 1$.

To find the dependence of ratio between L_1 and L_2 on the total luminosity, we variate the L_{tot} from 20 pb^{-1} to 200 pb^{-1} , and for each L_{tot} , we fit the variation of S_{m_τ} as shown in Fig. 4(a). Then from each fit curve, the minimum (that is L_1) can be found and

drawn in Fig. 4(b). The linear relation between L_1 and L_{tot} accommodates the fixed slope 0.75. This is easy to understand since the ratio L_1 to L_2 reflects the correlation between S_{m_τ} and S_ϵ which will remain the same regardless of the variation of the total luminosity.

3.3 Three-parameter fit

Based on the results of the preceding section, two parameters m_τ and ϵ can be determined by the optimized first and second points which are located respectively at $E_1 = 3.55379 \text{ GeV}$ and $E_2 = 3.595 \text{ GeV}$ with the ratio of luminosity between the two points fixed at 3 to 1. As to the new adding fit parameter σ_{BG} , we divide the luminosity 20 pb^{-1} into 1, 2, 3, 4 or 5 points with the energy ranging from 3.50 to 3.54 GeV (the luminosities for point 1 and 2 are $L_1 = 75 \text{ pb}^{-1}$ and $L_2 = 25 \text{ pb}^{-1}$). The fit results are shown in Fig. 5(a). It can be seen that the number

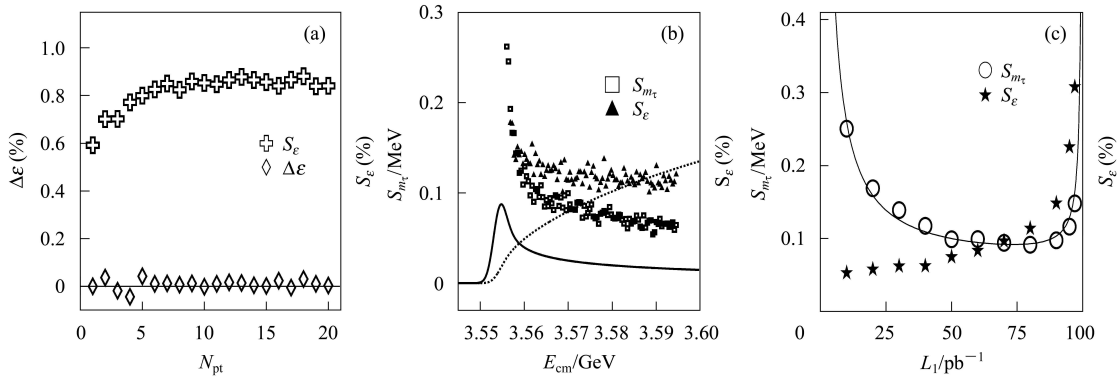


Fig. 3. (a) The variations of $\Delta\epsilon$ and S_ϵ with the number of points N_{pt} . (b) The variations of S_{m_τ} and S_ϵ with the scan of the second energy point from 3.554 to 3.595 GeV. The solid line denotes the derivative of cross section with the scale factor of 0.001 and the dotted line denotes the cross section with the scale factor of 0.1. (c) The variations of S_{m_τ} and S_ϵ with the increasing of L_1 .

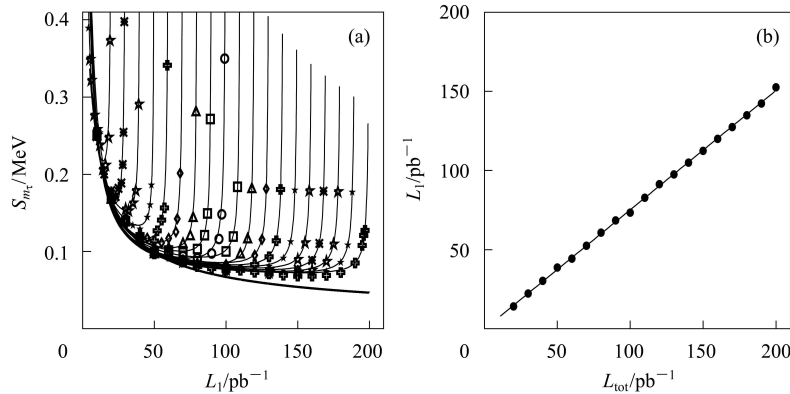


Fig. 4. The relation between S_{m_τ} and the total luminosity. (a) A series sets of S_{m_τ} vs. L_1 for different total luminosity L_{tot} variate from 20 pb^{-1} to 200 pb^{-1} with a step of 10 pb^{-1} . Overlaid are fits of functions with the form $A + B/(L - L_{\text{tot}}) + C/L$ based on which the minima of S_{m_τ} are obtained analytically. The bottom one is the S_{m_τ} vs. L curve in one-parameter fit case. (b) The optimal proportion of the luminosity allotted at the first energy point $E_1 = 3.55379 \text{ GeV}$ for different total luminosity L_{tot} .

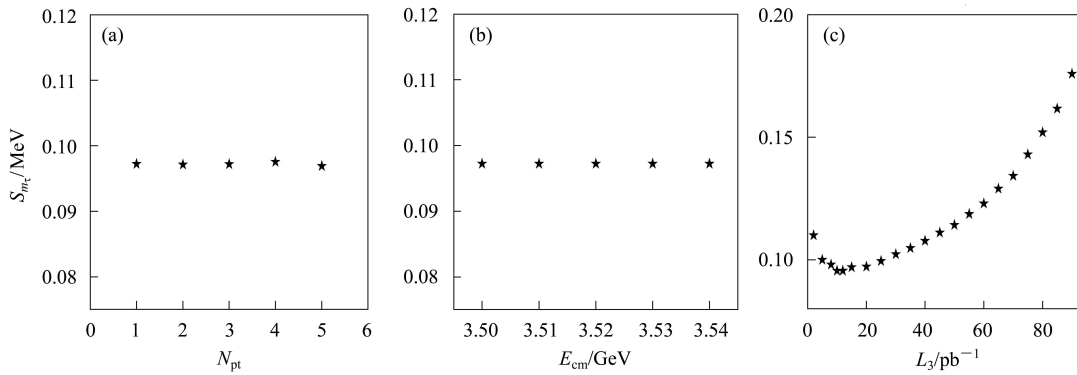


Fig. 5. The relation between S_{m_τ} and (a) the number of energy points N_{pt} . (b) the position of data taking point E_{cm} . (c) the luminosity at the third point L_3 .

of points has almost no effect on the fit uncertainty of m_τ or in other words, one point (denoted as the third point, E_3 , hereafter) is enough to determine the parameter σ_{BG} .

As the second step, with a luminosity of 20 pb $^{-1}$ for the third point, we perform the fit with $E_3 = 3.50, 3.51, 3.52, 3.53$, or 3.54 GeV, respectively. The relation between the S_{m_τ} and the energy position is shown in Fig. 5(b) which indicates that S_{m_τ} is almost irrelevant to energy, as long as it is below $\tau^+\tau^-$ threshold. As an example, $E_3 = 3.50$ GeV is chosen as the third point.

As the third step, we fix the total luminosity as 120 pb $^{-1}$, and then increase the proportion of the luminosity allotted at E_3 to find the dependence of S_{m_τ} on L_3 . As shown in Fig. 5(c), the smallest $S_{m_\tau} = 0.096$ MeV is obtained when the luminosity equals 12 pb $^{-1}$, which is about 10% of the total luminosity. That is to say $L_3 = 10\% \cdot L_{tot}$ together with $L_1/L_2 = 3$ will lead to the optimal value of S_{m_τ} .

4 Investigation of optimization

As pointed out in Ref. [14], the optimal number of points depends on the distribution of points and vice versa. Under the one-parameter fit case, the sampling technique is employed to take energy points randomly at the chosen interval, which in principle exhausts all possibilities and ensures the optimization of the final scheme. However, such a method is unfeasible for the multi-parameter fit due to the increasing complexity of the fit. For example, it is found when two energy points are too close to each other, the fit always fails for the two-parameter case. Fully corroborating the optimization of the aforementioned schemes is outside the scope of this paper. As a compromise, some possibilities are investigated to confirm the previous

optimal results.

As far as the two-parameter fit is concerned, the energy interval is divided evenly between $E_{cm} = 3.55$ and 3.5935 GeV for both E_1 and E_2 , then all possible combinations between E_1 and E_2 except for $E_1 = E_2$ are fitted, which will definitely lead to the failure of fit. For the ratio of L_1 to L_2 , three cases 1:1, 3:1, and 9:1 are tested¹⁾. The results for the case of $L_1/L_2 = 3$ are displayed in Fig. 6, according to which a few points could be noticed: 1) there exists a rough symmetry between E_1 and E_2 just as expected; 2) there are two valleys along the values of E_1 and E_2 near the m_τ threshold, which just correspond to the sensitive region for m_τ fit; 3) along each valley S_{m_τ} decreases gradually with the increasing of E_{cm} . All these points qualify the previous optimal scheme qualitatively.

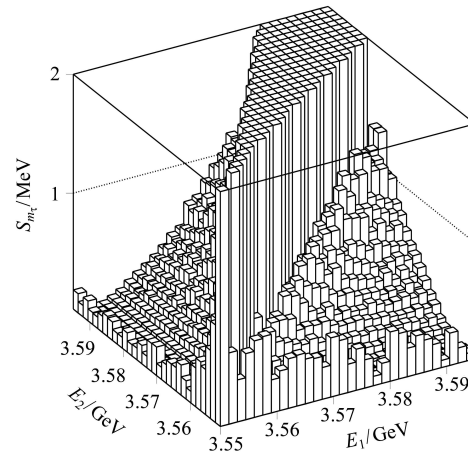


Fig. 6. The variation of S_{m_τ} with a 2 dimension scan of E_1 and E_2 in the energy region 3.55 ~ 3.595 GeV. The plateau is due to the adjacency between E_1 and E_2 which frequently leads to the failure of fit. (For such a case, S_{m_τ} is arbitrarily set to be a large value, say, 2 MeV or more).

1) Comparing the minimum of different luminosity ratios, it is found, the ratio 3:1 gives the minimal fit value of S_{m_τ} .

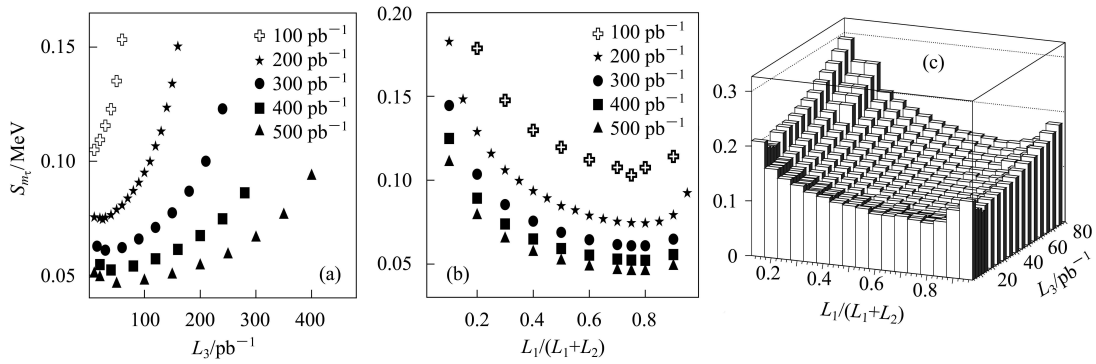


Fig. 7. The variation $S_{m\tau}$ with (a) L_3 . (b) the ratio of $L_1/(L_1+L_2)$. In (a) and (b), L_{tot} is extended from 100 to 500 pb^{-1} as illustrated in plots. (c) a two dimension scan of $L_1/(L_1+L_2)$ and L_3 , here, the total luminosity, $L_{\text{tot}} = L_1 + L_2 + L_3$, is fixed at 120 pb^{-1} .

When turning to the three-parameter fit, the problem seems more dazzled because of the more complex correlation among three parameters. However, intuitively the correlation among different points would be determined by the line shape of the cross section and has nothing to do with the total experiment luminosity. Therefore, it is natural to assume that the relative allocation of luminosity (determined by the correlation between parameters) remains the same with respect to the change of the total luminosity. Such a feature exhibits for two-parameter fit. To demonstrate the extensity of this point for three-parameter fit, two kinds of fit are performed, namely the relation between the $S_{m\tau}$ and L_3 as shown in Fig. 7(a) and the variation of $S_{m\tau}$ with the ratio of $L_1/(L_1+L_2)$ as shown in Fig. 7(b). As indicated in the two plots, the optimal values remain the same just as expected although the total luminosity enhances from 100 pb^{-1} to 500 pb^{-1} .

To consolidate our optimal scheme, for the fixed total luminosity, say $L_{\text{tot}} = 120 \text{ pb}^{-1}$, with $L_{\text{tot}} = L_1 + L_2 + L_3$, a two dimension scan of $S_{m\tau}$ is performed with respect to $L_1/(L_1+L_2)$ and L_3 and the results are presented in Fig. 7(c). Clearly, for the fixed L_3 , the smallest $S_{m\tau}$ is obtained at the value $L_1/(L_1+L_2) = 0.75$ while for the fixed ratio, the smallest $S_{m\tau}$ is obtained at the value $L_3 = 12 \text{ pb}^{-1}$, which is around 10% of the total luminosity. In fact, the smallest $S_{m\tau}$ can be read directly from the three-dimension plot, with the coordinates $L_1/(L_1+L_2) \approx 0.75$ and $L_3/L_{\text{tot}} \approx 10\%$. These values are just what are obtained in Section 3.3.

5 Suggestion on data taking

Using the optimization results obtained in Sec-

tion 3, the relations between L_{tot} and $S_{m\tau}$ for the two- and three-parameter fits are drawn in Fig. 8. In addition, the results for the one-parameter fit^[14] are presented for comparison. Obviously, the more parameters which need to be fit, the more the luminosity is required to acquire the same precision. However, the prominent merit for the three-parameter fit lies in the fact that the correlation among fit parameters is taken into account automatically by fit program¹⁾. Therefore, the following discussion is based on the results of the three-parameter fit.

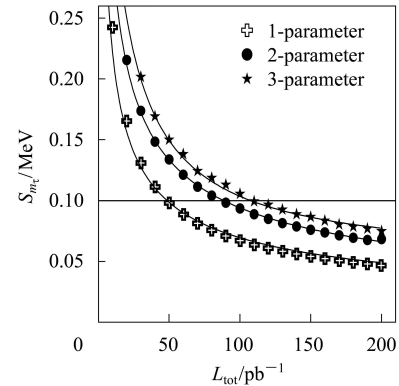


Fig. 8. Dependence of $S_{m\tau}$ on L_{tot} for one-, two- and three-parameter fit schemes. Overlaid are fits of functions with the form $A/L^{0.504}$.

The designed peak luminosity of BEPC II is $10^{33} \text{ cm}^{-1} \cdot \text{s}^{-1}$ for $E_{\text{beam}} = 1.89 \text{ GeV}$ ^[15]. If the averaged efficiency of luminosity is taken as 50% of the peak value, no more than three days data taking can lead to the precision of $S_{m\tau}$ less than 0.1 MeV. It should be noticed here that this evaluation is merely

1) In principle, one- and two-parameter fits could also be adopted. However, the correlation between the fitting parameters and fixed parameter(s) should be considered separately, which is actually a complicated and time-consuming process. Therefore, from the point view of error analysis, the three-parameter fit scheme is more favorable.

on a basis of $e\mu$ tagged events, according to the previous BES result^[3], the number of multi-channel-tagged (such as ee , $e\mu$, eh , $\mu\mu$, μh , hh , where h denotes hadron) events is at least five times more than those of the $e\mu$ tagged events. If more channels are utilized to tag τ -pair final states, more statistics can be expected.

To measure the m_τ with high accuracy at BESIII, at least three points are needed for the data taking. The first point with $L_1 = 67.5\% \cdot L_{\text{tot}}$ is at the large derivative region, which mainly affects the precision of m_τ ; the second point with $L_2 = 22.5\% \cdot L_{\text{tot}}$ is above the threshold, which can be used to study the efficiency of the event selection; and the third point with $L_3 = 10.0\% \cdot L_{\text{tot}}$ is below the threshold, which is crucial for the background determination.

From the point view of BESIII physics analysis, the data taken above and below the m_τ threshold can also be utilized for R -value measurement and background study of J/ψ and ψ' physics. Therefore, maybe many more data are needed at Point 2 and 3. As a matter of fact, if the branching ratio measurement of τ decay is taken into account, a considerably large data sample is needed at the m_τ threshold as indicated in Ref. [16]. All these considerations indicate that a more detailed and systematic plan is required

for the actual data taking in the future.

6 Summary

The statistical uncertainty of m_τ measurement at BESIII is studied in great detail. Three cases, that is the one-, two-, and three-parameter fit, are considered and the optimization for each fit case is realized by virtue of Monte Carlo simulation and sampling technique. The study reveals some prominent and/or special characters of m_τ measurement. First, the fit results indicate that one energy point is sufficient to determine one fit parameter. Second, the luminosity proportion distributed at different energy points for the multi-parameter fit is almost fixed and independent of the total luminosity. Third, a certain energy point is more sensitive to one special parameter than to the others. Furthermore, the optimal scheme for each fit case is reinforced by checking various possibilities and comparing a great number of fit results.

The suggestions on the data taking for m_τ measurement are put forth based on the conclusion of the three-parameter fit. Moreover, some practical requirements for data taking are also discussed from the viewpoint of BESIII physics.

References

- 1 Albrecht H et al. (ARGUS Collaboraton). Phys. Lett. B, 1992, **292**: 221
- 2 Belous K et al. (Belle Collaboration). Phys. Rev. Lett., 2007, **99**: 011801
- 3 BAI J Z et al. (BES Collaboration). Phys. Rev. D, 1996, **53**: 20
- 4 BAI J Z et al. (BES Collaboration). Phys. Rev. Lett., 1992, **69**: 3021
- 5 BAI J Z et al. (BES Collaboration) HEP & NP, 1992, **16**: 343
- 6 Bogomyagkov A et al. Research of Possibility to Use Beam Polarization for Absolute Energy Calibration in High-precision Measurement of Tau Leptonic Mass at VEPP-4M. 9th European Particle Accelerator Conference. Lucerne, Switzerland, 2004
- 7 Voloshin M B. Phys. Lett. B, 2003, **556**: 153
- 8 Smith B H, Voloshin M B. Phys. Lett. B, 1994, **324**: 177
- 9 Pich A. Perspectives on Tau-Charm Factory Physics. Proceedings of the 3rd Workshop on the Tau-Charm Factory. Marbella, Spain, 1993, 767
- 10 Femenia P R, Pich A. Phys. Rev. D, 2001, **63**: 053001
- 11 BES Collaboration. The BESIII Detector. 2004
- 12 YAO W M et al. Journal of Physics G, 2006, **33**: 1
- 13 Brandt S. Data Analysis. 3rd ed. New York: Springer-Verlag, 1999
- 14 WANG Y K, MO X H, YUAN C Z et al. Nucl. Instrum. Methods A, 2007, **583**: 479—484
- 15 Design Report of Accelerator BEPCII (Accelerator Part). 2002. http://acc-center.ihep.ac.cn/download/pdr_download.htm
- 16 HUA C F, MO X H, LI Y X et al. Nuclear Electronics & Detection Technology, to be published (in Chinese)